Local-regional similarity in drylands increases during multiyear wet and dry periods and in response to extreme events

M. D. PETRIE,[1],† D. P. C. PETERS,[2,3] N. D. BURRUSS,[3] W. JI,[4] AND H. M. SAVOY[3]

[1]School of Life Sciences, University of Nevada Las Vegas, Las Vegas, Nevada, USA
[2]United States Department of Agriculture - Agricultural Research Service, Jornada Experimental Range, Las Cruces, New Mexico, USA
[3]Jornada Basin LTER Program, New Mexico State University, Las Cruces, New Mexico, USA
[4]Department of Plant & Environmental Sciences, New Mexico State University, Las Cruces, New Mexico, USA

Abstract. Climate change is predicted to impact ecosystems through altered precipitation (PPT) regimes. In the Chihuahuan Desert, multiyear wet and dry periods and extreme PPT pulses are the most influential climatic events for vegetation. Vegetation responses are most frequently studied locally, and regional responses are often unclear. We present an approach to quantify correlation of PPT and vegetation responses (as Normalized Difference Vegetation Index [NDVI]) at the Jornada ARS-LTER site (JRN; 550 km^2 area) and the surrounding dryland region (from 0 to 500 km distance; 400,000 km^2 study area) as a way to understand regional similarity to locally observed patterns. We focused on fluctuating wet and dry years, multiyear wet or dry periods of 3–4 yr, and multiyear wet periods that contained one or more extreme high PPT pulses or extreme low rainfall. In all but extreme high PPT years, JRN PPT was highly correlated ($r > 0.9$) to PPT across the regional study area (0–500 km distance; high correlation from 25th to 75th percentiles) and was highly correlated across a greater PPT range subregionally (0–200 km distance; high correlation from 10th to 90th percentiles). In contrast, the statistical distribution of JRN NDVI was less similar to that of regional NDVI. Yet, local-regional NDVI similarity increased during multiyear periods to a maximum of >90% similarity for 10th–90th percentiles in a number of years. Thus, local-regional heterogeneity in PPT and vegetation responses is reduced in both multiyear wet and dry periods, with the largest changes in climatic forcing and responses during multiyear wet periods. These wet and dry events support greater similarity between local-regional PPT and vegetation response patterns. We conclude that site-based research on multiyear periods can be extended to anticipate larger regional responses, and illustrate the opportunity to enhance understanding of future PPT change through increased focus on multiyear periods.

† **E-mail:** matthew.petrie@unlv.edu

INTRODUCTION

There is considerable need to extend local ecological observation and insight to better understand broad regions of similar ecosystem types (Foley et al. 2000, Peters et al. 2014), especially vegetation responses to influential precipitation (PPT) patterns (Knapp et al. 2017). In the American southwest, PPT has received substantial scientific attention, with recent research focusing on

scenarios of climatic change effects to aridity and extreme drought (Cook et al. 2015, Scott et al. 2015), seasonal PPT effects (Forzieri et al. 2011, Notaro and Gutzler 2012), and the influence of PPT patterns on vegetation productivity and other ecological processes (Sala et al. 2012, Estiarte et al. 2016). However, studies focusing on spatiotemporal PPT effects across broad regions are relatively rare (Brunsell and Young 2008, Mendez-Barroso et al. 2009 and Zhang et al. 2011 for exceptions in other regions), and the local- to regional-scale relationships between climate and vegetation responses in the American southwest remain uncertain.

Climate change is predicted to increase temperatures across the American southwest, with effects on regional aridity that will be shaped by PPT (Mueller and Seneviratne 2012, Cook et al. 2015, Lehner et al. 2018). Projections for PPT are more uncertain than those of temperature in this region and may include a combination of small changes in seasonal rainfall and/or increasing inter- and intra-annual variability (Gutzler and Robbins 2011). PPT changes could therefore result in wetter conditions, drier conditions, and/or more variable conditions, although a more arid future with enhanced drought is most likely (Cayan et al. 2010, Cook et al. 2015). Predicting the possible effects of these changes is challenging because dryland vegetation responds to multiple factors including current-year conditions, legacy effects of past conditions, and biotic and abiotic landscape factors (Duniway et al. 2010a, Peters et al. 2014, Gherardi and Sala 2015, Petrie et al. 2018). Vegetation is also sensitive to temporal PPT patterns and to extreme PPT events, which fluctuate over time periods of days to multiple years (Jentsch and Beierkuhnlein 2008, Collins et al. 2014 for an overview of extreme events and pulse dynamics). The way that these responses differ across larger and more heterogeneous areas is even less understood. For this reason, there is need to determine whether and to what degree multifactor effects and vegetation responses are similar across dryland regions.

Vegetation at the Jornada Long Term Ecological Research and Agricultural Research Service site (JRN LTER-ARS) in the northern Chihuahuan Desert is highly sensitive to extended periods of above-or below-average PPT (i.e., multiyear wet and dry periods), especially herbaceous vegetation which responds strongly to both wet and dry periods (Swetnam and Betancourt 1998, Peters et al. 2012, 2014). For example, a 2004–2008 multiyear wet period at JRN reversed the effects of a prior extreme drought from 2000 to 2003 and instigated substantial herbaceous vegetation recovery that was not observed in preceding wet periods (Peters et al. 2012). Wet and dry periods have important consequences for other central and western North American ecosystems, with effects to vegetation that may aggregate over multiple years (Sala et al. 2012, Petrie et al. 2018). To better understand these multiyear events, a growing area of research focuses on experimentally manipulating sustained extreme high and low PPT in a field setting (Fay et al. 2000, Collins et al. 2012, Hoover and Rogers 2016), and recent network development is targeting extreme drought manipulations across global ecosystems (Knapp et al. 2017). Despite the growing consensus that multiyear periods are important, their regional effects have largely been inferred from results and observations at a single location. We postulate that this tendency may overemphasize the representativeness of a single location and oversimplify the multifactor relationships governing vegetation responses, especially if regional biotic and abiotic factors differ from those observed locally.

Teleconnections are most commonly used in atmospheric science to relate mechanistic relationships between forcing conditions and response events, such as sea surface temperature anomalies to climate patterns associated with the El Nino Southern Oscillation (Alexander et al. 2002). Ecoclimate teleconnections explore feedbacks between climate and ecological change, where climate-initiated ecological change in one location initiates future change in a different location or across a broader region. Examples of ecoclimate teleconnections include regional soil moisture-precipitation feedbacks in the Great Plains (Brunsell and Wilson 2013), increasing regional aridity following large-scale forest mortality events and surface albedo (Garcia et al. 2016, Stark et al. 2016), and feedbacks between deforestation and rainfall in tropical forests (Sternberg 2001). Building on the framework of understanding local-regional similarity and the occurrence of change in climatic driver and
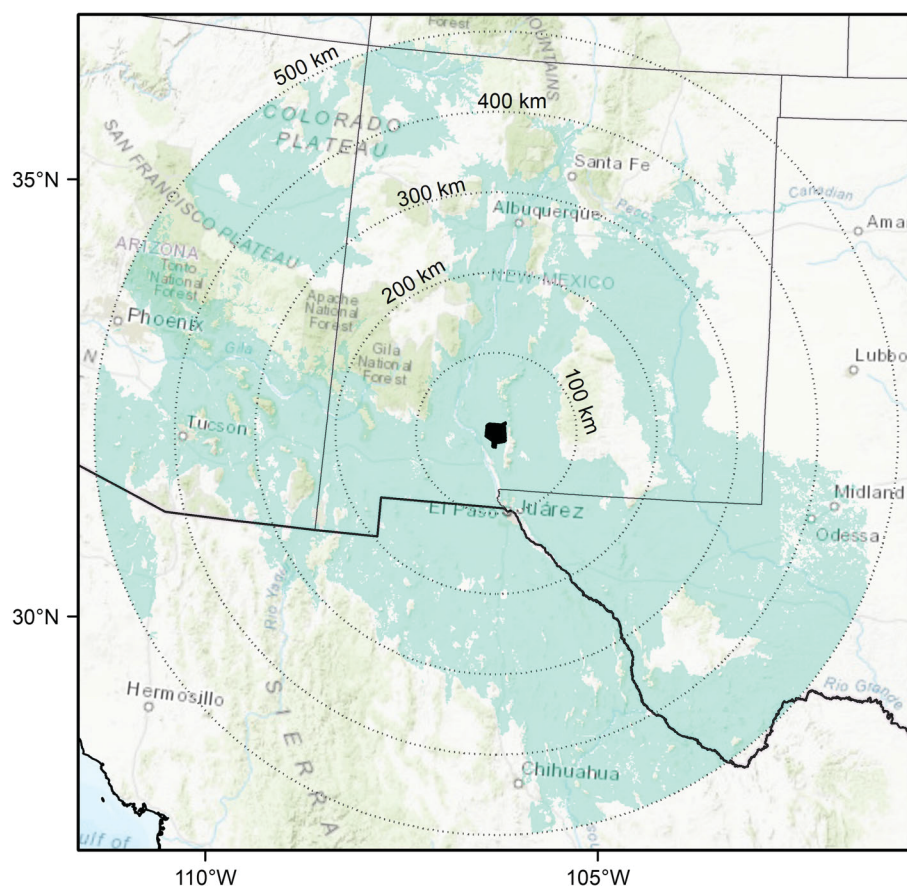
Fig. 1. Study area map with study area in blue and the Jornada ARS-LTER site in the center. The analysis was iterated outwardly from JRN incrementally from 0 to 500 km radial distance.

vegetation response patterns, we propose a tele-connections-based approach that supports the determination of how representative a field site is of its larger region, and helps to elucidate to what degree local insight may also inform understanding of regional processes. We propose that this approach can be used in a stepwise manner; for example, better understanding of the local-regional extent of PPT and vegetation response patterns can guide additional research on similarity in the factors shaping local-regional responses (Petrie et al. 2019). In this way, it is possible to provide a framework to guide extension of local insight and prediction of future regional conditions that are developed through observation at multiple scales.

Prior multiyear periods provide foresight on the conditions required for local-regional similarity to increase. The most well documented of

these periods in the American southwest is the early 2000s global-change-type drought and its effects on semiarid woodlands. This drought occurred from ~2000 to 2003 and instigated widespread regional tree mortality beginning in 2002 and 2003, which occurred locally from as few as 15 months of moisture limitation (Breshears et al. 2005, 2009). Variation in the timing of mortality (2002, 2003) shows that drought impacts took multiple years to be realized across the region (Williams et al. 2002, Breshears et al. 2009). Thus, even the most substantial extreme multiyear drought of the past 50 yr—a low-variance forcing scenario of low PPT and extreme high temperatures that occurred across a broad region—did not have substantial effects on vegetation mortality until the 3rd or 4th consecutive dry year. Based on these findings, we postulate that for a multiyear dry or wet period to have

Table 1. Site summary for the Jornada ARS-LTER site (JRN) and for areas 0–100 km to 0–500 km from the JRN centroid.

Location	Study area [km^2]	Elevation [m]	April–September PPT [mm]	April–September NDVI maximum (50th percentile)
JRN	552	1371 ± 60	179	0.20
0–100 km	27,329	1398 ± 171	177 (−1%)	0.20
0–200 km	62,750	1439 ± 222	184 (+3%)	0.21 (+5%)
0–300 km	110,942	1391 ± 267	204 (+14%)	0.24 (+20%)
0–400 km	90,371	1322 ± 358	206 (+15%)	0.24 (+20%)
0–500 km	105,527	1192 ± 418	203 (+13%)	0.24 (+20%)

Table 2. Data sources.

Variable	Source resolution	Analysis resolution	Time period	Source	Location
Precipitation	1 km^2	1 km^2	1980–2016	DayMet v.3	http://dx.doi.org/10.3334/ORNLDAAC/1219
Land cover	250 m^2	1 km^2	Static	NALCMS	https://landcover.usgs.gov/nalcms.php
Elevation	1 km^2	1 km^2	Static	GTOPO30	https://lta.cr.usgs.gov/GTOPO30
NDVI	30 m^2	1 km^2	1984–2016	Landsat	https://landsat.gsfc.nasa.gov/

Note: NDVI, Normalized Difference Vegetation Index.

widespread regional impacts, it must constitute a significant change to PPT magnitude and must also occur for a sustained period of time to allow for vegetation responses to aggregate across space. In drylands that normally experience high PPT stochasticity from convective rainfall events (Petrie et al. 2014), we further postulate that multiyear wet periods reduce local-regional PPT variability because they experience widespread prolonged rainfall, whereas dry periods reduce local-regional PPT variability because very little rainfall occurs. As a result, variability in vegetation responses is ultimately reduced in both multiyear wet and dry periods, but for different reasons.

We sought to develop insight on the local-regional patterns of multiyear wet and dry periods between JRN and the Chihuahuan Desert region, to characterize the pattern and impact of these periods, and to better understand how local ecological insight might be extended regionally. To do this, we quantified correlations between statistical distributions of PPT and vegetation responses (as Normalized Difference Vegetation Index [NDVI]) at JRN (550 km^2 area) to those across the Chihuahuan Desert region of the United States and Mexico (from 0 to 500 km distance; 400,000 km^2 study area). Our analysis focused on PPT periods observed locally at JRN: fluctuating wet and dry years corresponding to average PPT conditions, multiyear wet and dry periods of 3–4 yr in length, and multiyear wet and dry periods that contained one or more extreme pulses of high PPT or an extreme dry year, respectively. Our goals were to (1) determine how representative statistical distributions of PPT and NDVI at JRN are of those across a larger dryland region under average conditions of fluctuating wet and dry years and (2) evaluate and contrast local-regional PPT and NDVI correlations during multiyear wet and dry periods in the context of their deviation from average conditions. We hypothesized that regional PPT and NDVI would have low local-regional correlation under average conditions due to high PPT stochasticity from local convective rainfall events and high vegetation heterogeneity, but that local-regional correlation would increase during multiyear periods as PPT stochasticity became more homogenized and vegetation responses became more similar. Due to their lower PPT variance, we expected that multiyear dry periods would be the most highly correlated periods for vegetation due to low NDVI across the region.
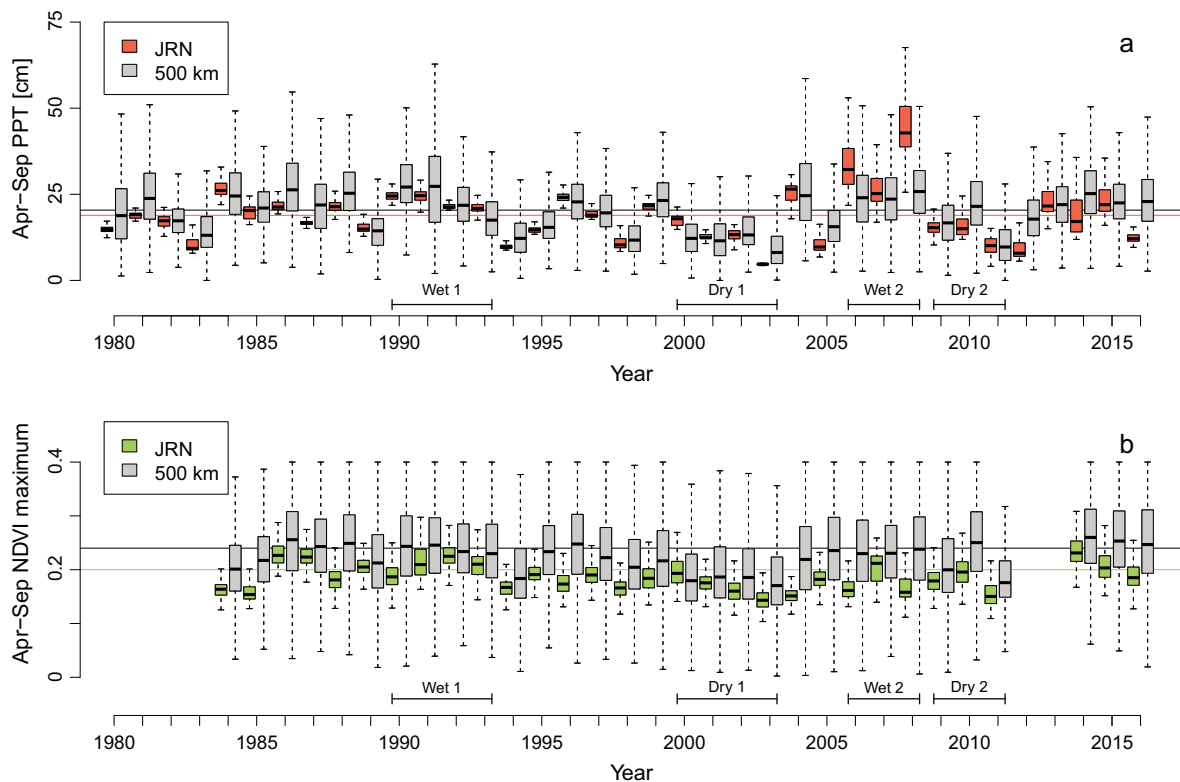
Fig. 2. Timeseries of April–September total precipitation [PPT: cm] between JRN (red) and 0–500 km distance study area cells (gray; a), and timeseries of April–September maximum Normalized Difference Vegetation Index (NDVI) values between JRN (green) and 0–500 km distance study area cells (gray; b). All multiyear dry and wet periods are labeled. Maximum NDVI values were low in 2006 and 2008 due to high cloud cover and were not available in 2012 and 2013.

SITE DESCRIPTION

We compared growing season (April–September) PPT and vegetation responses between JRN (32.5° N, 106.8° W) in southern New Mexico, USA, and the Chihuahuan Desert region of the United States and Mexico (Fig. 1). PPT totals during the April–September growing season are most highly correlated to vegetation productivity in the Chihuahuan Desert, and this is the period during which extreme PPT pulses are most likely to occur (Petrie et al. 2014, 2018). Average growing season PPT from 1980 to 2016 across the JRN study area was ~179 mm, 70–80% of the annual total. Growing season totals averaged across the regional study area were slightly higher (203 mm; +13%; Table 1). Average daily temperature at the JRN Headquarters Weather Station was 14.9 ± 8.0°C, with an average high of 26.2°C in July. Vegetation

at JRN is characteristic of the Chihuahuan Desert region and includes black grama-dominated grasslands (*Bouteloua eriopoda*), and shrublands dominated by creosotebush (*Larrea tridentata*), honey mesquite (*Prosopis glandulosa*), and tarbush (*Flourensia cernua*). Regional vegetation is classified as temperate-subtropical and temperate-subpolar grasslands and shrublands, similar to that of JRN (Table 2). These vegetation types begin to change from 400 to 500 km distance from JRN (Fig. 1) into vegetation types typical of the Sonoran Desert (Arizona, USA, and Sonora, MX), Colorado Plateau grassland and shrubland (Arizona and New Mexico, USA), Great Plains grassland and shortgrass steppe (New Mexico and Texas, USA), and subtropical grassland and shrubland (Chihuahua, MX).

JRN has experienced a number of meaningful PPT-driven climatic events over the past century.
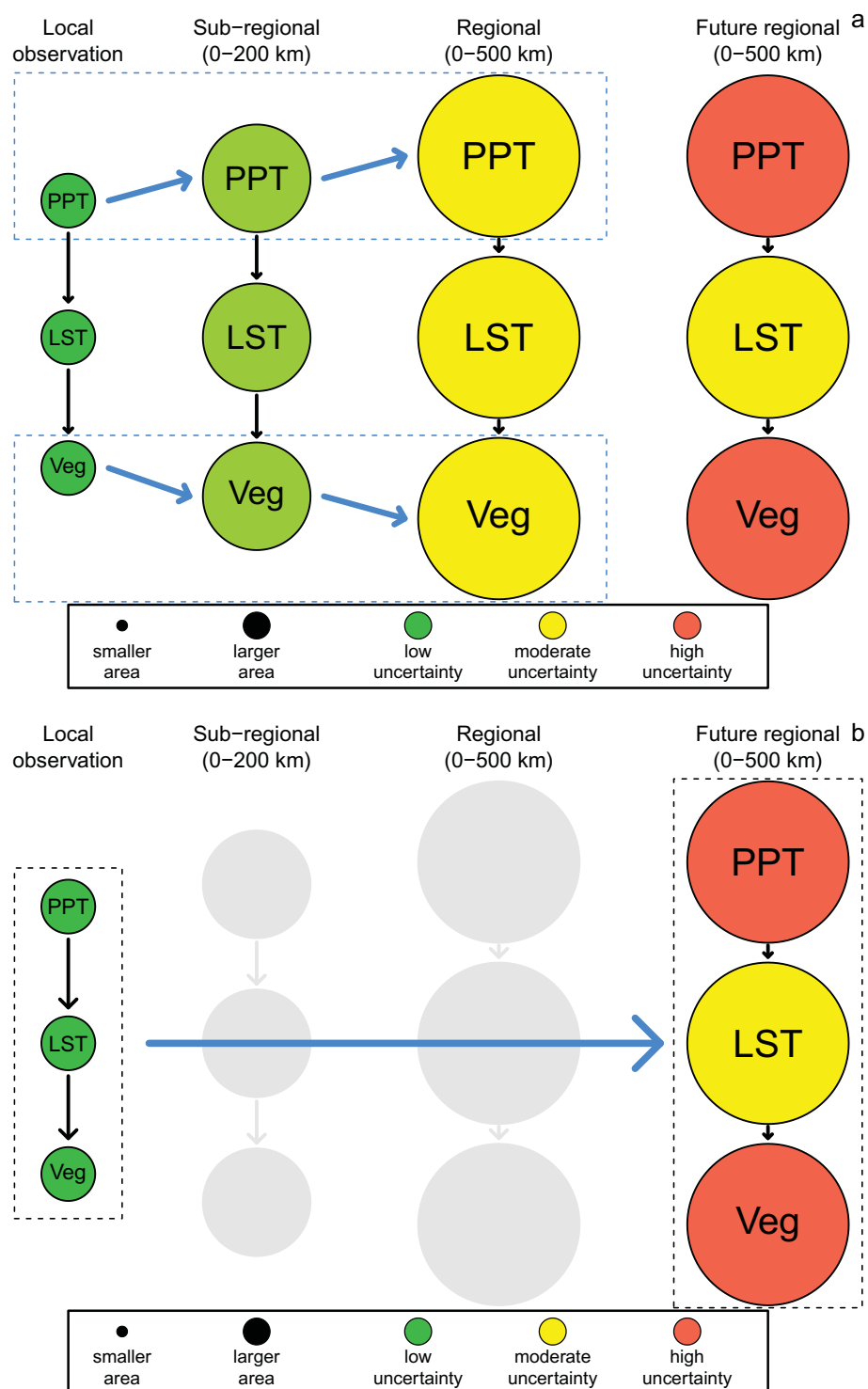
Fig. 3. Schematic of our approach. Vegetation responses (Veg) are influenced by precipitation (PPT) patterns and Land Surface Template (LST) conditions. The multifactor effects of PPT and LST vary across spatial scales; local effects are often observable directly and therefore have low uncertainty, whereas subregional and regional

(Fig. 3. *Continued*)
effects are more uncertain. Our goal in this study (indicated by blue boxes and arrows) was to better understand similarity between local-regional PPT and vegetation responses (a). The ultimate goal of this research is to understand how local insight can be used to sharpen regional prediction (b).

We were particularly interested in two multiyear wet periods and two multiyear dry periods that occurred over our 1980–2016 study period, which corresponds to the time span of continuous long-term data collection at JRN (1980) and availability of satellite data (1983). The first wet period (Wet 1: 1990–1993) experienced above-average JRN and regional PPT, whereas the second (Wet 2: 2006–2008) was punctuated by extreme high growing season PPT pulses in 2006 and 2008. The first dry period (Dry 1: 2000–2003) was a regional drought with an extreme dry year in 2003, and the second (Dry 2: 2009–2012) was less-severe and more regionally variable (Fig. 2a). Vegetation productivity responses at JRN track rainfall during these periods (Petrie et al. 2018), with some variation due to land surface properties and spatial PPT variability (Peters et al. 2014).

METHODS

Local-regional similarity

Our approach focuses on the development of a stepwise framework to understand PPT patterns, land surface template (LST) conditions, and vegetation responses (PPT-LST-Veg) across broad regional areas (Fig. 3a). Uncertainty in PPT-LST-Veg varies across spatial scales; local effects may often be observed in situ and have relatively low uncertainty, whereas subregional and regional effects that are not observed directly have higher uncertainty. It is also not clear to what degree locally observed patterns of PPT and vegetation responses are similar to those across regional areas (moving from left to right in Fig. 3a), and how these relationships change under differing PPT forcing events, such as multiyear periods. Our goal in this study (highlighted by blue boxes and arrows in Fig. 3a) was to better understand similarity between the distribution of local-regional PPT and vegetation responses under average PPT forcing conditions and during multiyear wet and dry periods. To do this, we compared the correlation (PPT) or similarity (Veg) of percentile-determined groups of pixels locally at JRN to

those across varying distances across the Chihuahuan Desert region (from a radius of 0–50 km to one of 0–500 km). These analyses support the determination of how representative observations at JRN are of the larger Chihuahuan Desert region, and how local-regional heterogeneity in PPT and Veg differs and changes during multiyear PPT forcing events. The ultimate goal of this research is to sharpen prediction of future PPT-LST-Veg relationships regionally under scenarios of future climate change (Fig. 3b).

Study area delineation

Our study region was comprised of 1 km^2 cells within a 500 km radius from the center of JRN, an area of ~785,000 km^2 that we filtered to an effective study area of ~400,000 km^2 (Fig. 1). Included cells in our study were ≤2000 m in elevation, with ≥90% of land cover classified as temperate or subtropical grassland/shrubland, or barren (see Table 2 for a summary of these data sources). Included cells had an average growing season rainfall ± one standard deviation from the 1980–2016 JRN mean (179 ± 86 mm). Because land cover may differ from North American Land Change Monitoring System (NALCMS) data or may have changed over our study period, we only included cells with NDVI ≤ 0.4 in each year, which corresponds to a break point between desert vegetation and other land cover types in this region. We evaluated multiple NDVI break points from 0.3 to 0.5 over our analysis years to verify that desert cells with high vegetation responses were not removed from the analysis. All data were transformed to conform to a 1 km^2 reference grid using bilinear interpolation. All geospatial analyses were conducted using ArcGIS 10.4 (ESRI 2018) and R Project for Statistical Computing software (R Development Core Team 2016).

Precipitation and NDVI

We obtained total monthly PPT totals from DayMet v.3 interpolated data for North America (Table 2) and calculated growing season (April–
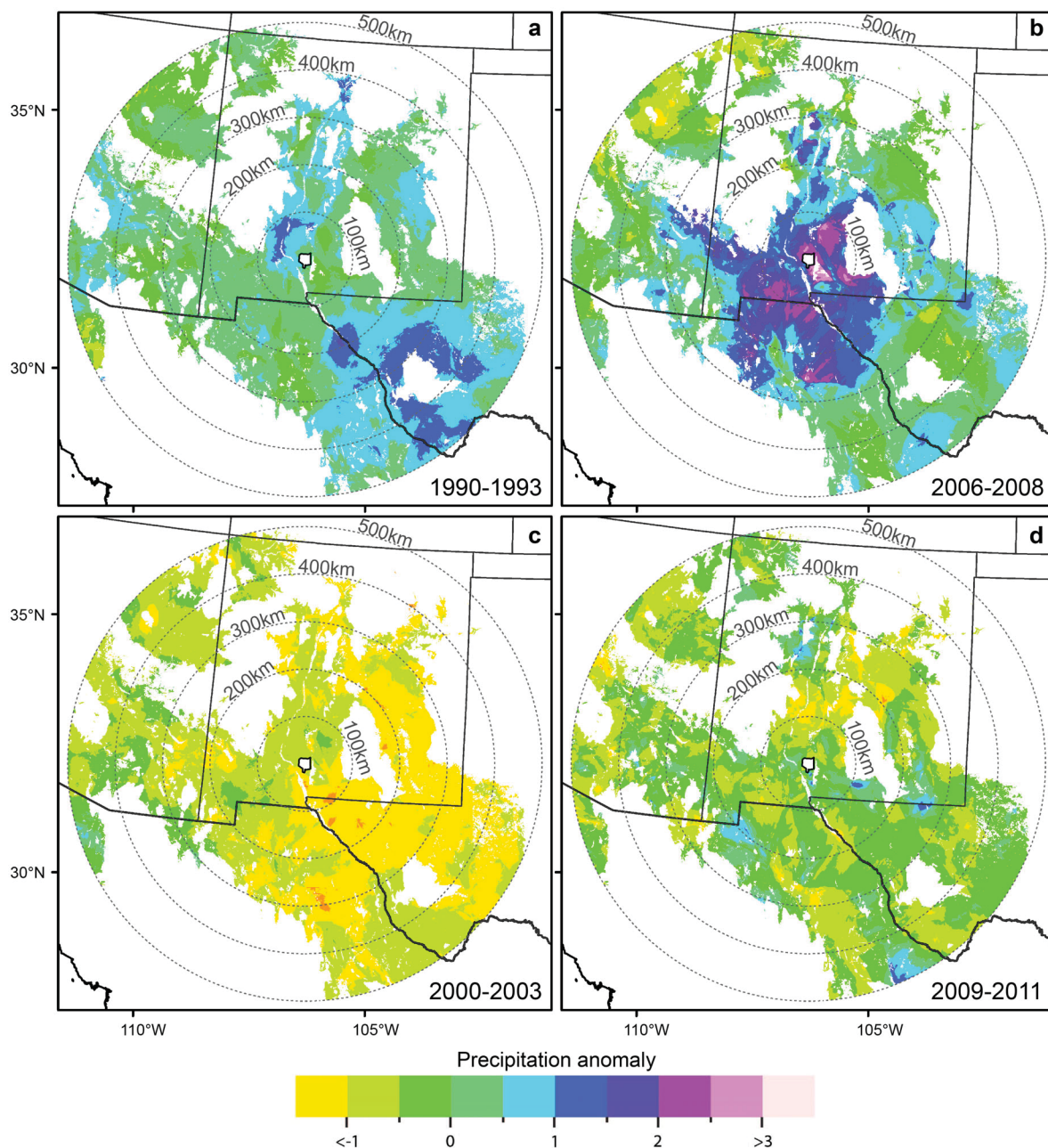
Fig. 4. Maps of average April–September precipitation anomaly [Pa: (observed-mean)/(SD)] for the 1990–1993 (a) and 2006–2008 (b) multiyear wet periods, and for the 2000–2003 (c) and 2009–2011 (d) multiyear dry periods.

September) totals for 1980–2016. Because average PPT in each cell differed, we calculated the yearly PPT anomaly from the long-term (1980–2016) mean and standard deviation of growing season rainfall at each cell (Pa = observed–mean/SD). We defined multiyear PPT as periods at JRN with consecutive years of sustained above-average or below-average rainfall totals. We obtained NDVI data from Landsat from 1984 to 2016 and used observed maximum NDVI from April to September in each cell for our analyses (Table 2). NDVI data in 2012–2013 were not available, and JRN

Table 3. Summary of precipitation anomaly (Pa) and maximum Normalized Difference Vegetation Index (NDVI) for the multiyear wet and dry periods of our study.

| Variable | 1990–1993: wet | | 2006–2008: wet | | 2000–2003: dry | | 2009–2011: dry | |
	JRN	0–500 km	JRN	0–300 km	JRN	0–500 km	JRN	0–500 km
Pa	0.53 ± 0.22	0.40 ± 0.38	2.04 ± 0.35	0.93 ± 0.66	−0.83 ± 0.08	−0.91 ± 0.30	−0.63 ± 0.25	−0.40 ± 0.38
NDVI	0.21 ± 0.02	0.24 ± 0.06	–	0.25 ± 0.08	0.17 ± 0.02	0.19 ± 0.06	0.18 ± 0.02	0.22 ± 0.06

Note: NDVI measurements were low regionally in 2006 and 2008 due to high cloud cover, and unavailable for JRN.
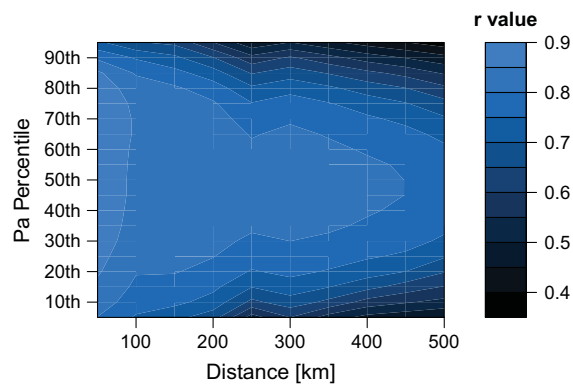

Fig. 5. Plot comparing JRN Pa percentiles (5th to 95th; JRN values–region values) from 1980 to 2016 to the same Pa percentiles from cells 0–50 km to 0–500 km distance from JRN, excluding the 2006 and 2008 extreme rainfall years which differed strongly between JRN and the larger region. The color ramp indicates the modified version of Mielke's *r*, which compares JRN to regional Pa percentiles over multiple distances. An example analysis with a single Pa and single distance is in Appendix S1: Fig. S1.

observations were artificially low in 2006 and 2008 due to cloud cover associated with high rainfall. Because NDVI data were not available in 2012, we limited our analysis of Dry 2 to 2009–2011.

Analysis

We compared the percentile distributions of gridded cells of PPT and NDVI at JRN to percentile distributions across the larger study area incrementally, moving outward from JRN by radial distance (from 0 to 50 km to 0 to 500 km) to determine local-regional (JRN-Chihuahuan Desert region) correlation (for PPT) and 90% similarity (for NDVI). These analyses are based on comparison of interpolated dependent variables

(PPT and NDVI). To compare JRN PPT to regional values, we correlated the 5th to 95th percentiles of JRN precipitation anomaly (Pa) to the same percentiles across distances from JRN (from 0 to 50 km to 0 to 500 km). Reported *r* values for each percentile of Pa were calculated using a modified version of Mielke's *r* from Duveiller et al. (2015), which reduces the *r* correlation coefficient in response to additive and multiplicative biases, instead of major-axis regressions or slope–intercept techniques, which are less-adept at accounting for these biases (Mesple et al. 1996, Pineiro et al. 2008). As a result, our reported *r* values are lower than more typically used *r* values, but provide a more complete correlation assessment with fewer biases. Similarity analysis of NDVI focused on local-regional raw NDVI percentile values that were 90% similar (e.g., is the 5th percentile of JRN NDVI 90% similar to the 5th percentile of regional NDVI across different distances?). This allowed us to determine to what degree the distributions of local-regional NDVI were similar without suggesting that these patterns were predictable, which requires understanding the role of additional factors. To summarize local-regional NDVI similarity across all distances as a single value, we calculated the percent area of the distributed NDVI values that were at least 90% similar, where a similarity in total value of 100% would indicate that all NDVI percentiles (5th to 95th) were 90% similar across all spatial ranges (0–50 km to 0–500 km). All statistical analyses were conducted using R (R Development Core Team 2016).

Results

Local-regional PPT and summary of multiyear periods

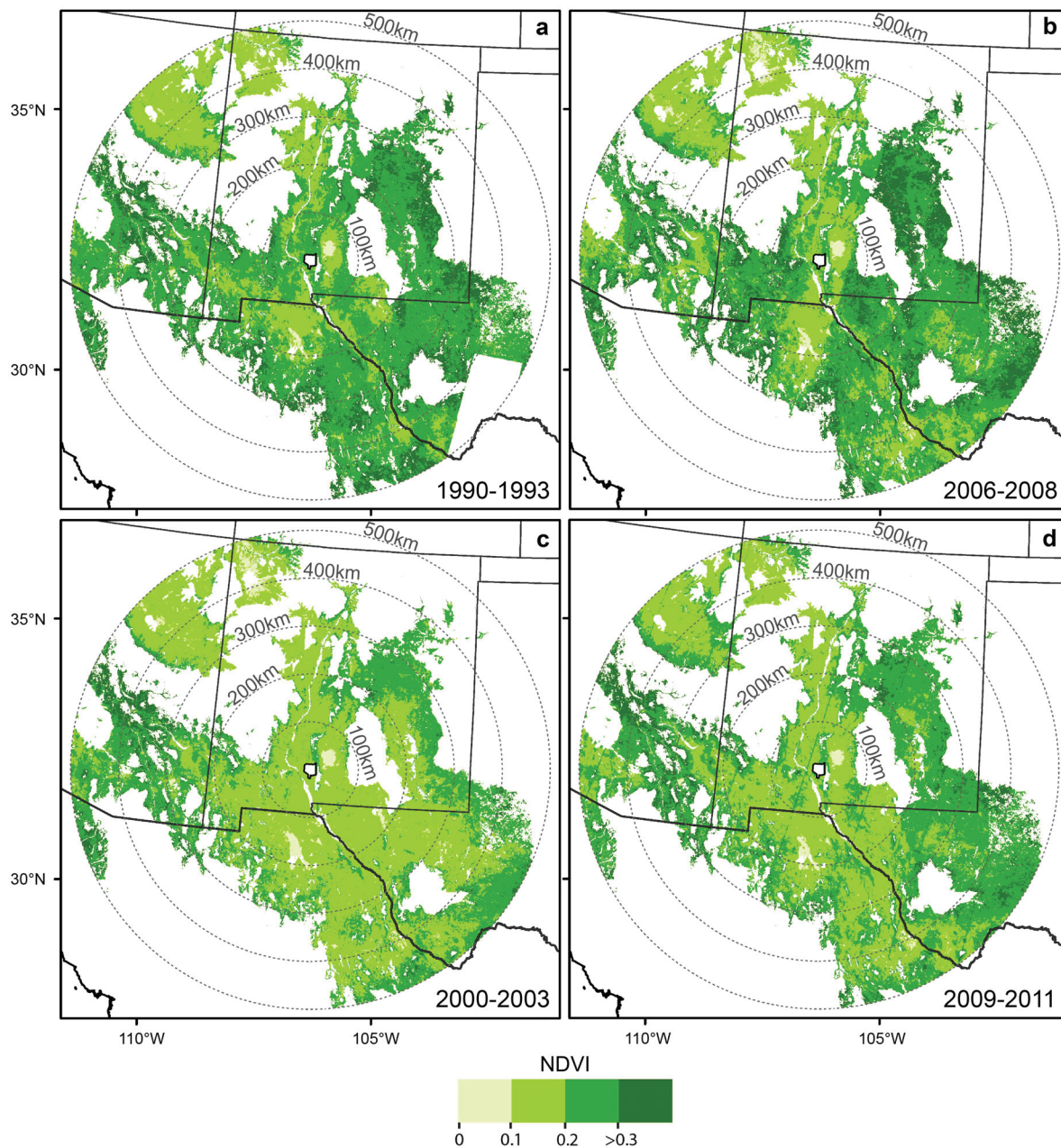Growing season PPT at JRN was slightly higher than the 0–500 km region in above-

Fig. 6. Maps of average April–September average maximum Normalized Difference Vegetation Index (NDVI) values for the 1990–1993 (a) and 2006–2008 (b) multiyear wet periods, and for the 2000–2003 (c) and 2009–2011 (d) multiyear dry periods.

average PPT years, was both higher and lower in below-average years, and had lower PPT variability (Fig. 2a, Table 1). This is due to the smaller area of JRN and our JRN-focused determination of wet and dry years, which did

not always correspond to regional PPT (Table 1). The multiyear wet and dry periods of our study had PPT patterns that differed from long-term mean values across the entire 0–500 km region, with the exception of 2006–2008 differed mainly
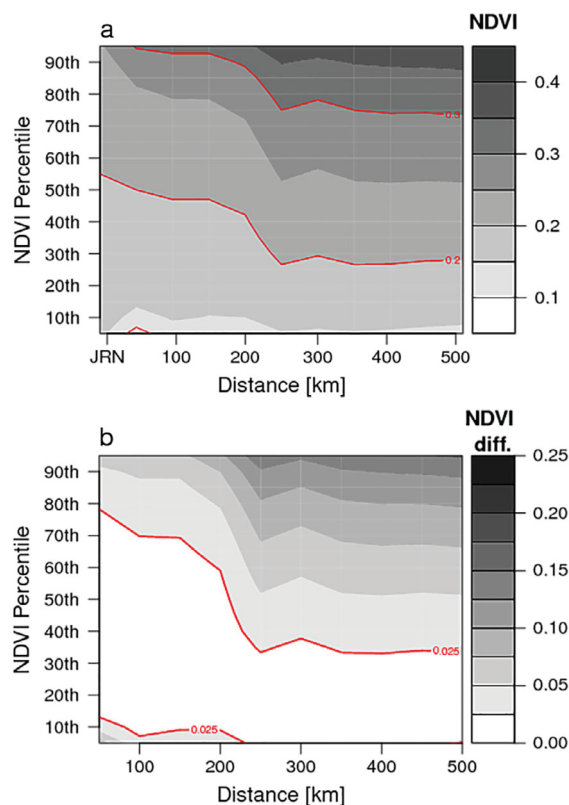
Fig. 7. Plots of raw NDVI between JRN cells and cells 0–50 km to 0–500 km distance from JRN (a), and differences in NDVI (organized as percentiles from 5th to 95th) between JRN cells and cells 0–50 km to 0–500 km distance from JRN (b). Both plots only include values in years not part of a multiyear wet or dry period. The red lines in Panel b indicate the thresholds above and below which JRN and regional cells have <0.025 (~90%) similarity.

from 0 to 300 km (Fig. 4; Appendix S1: Table S1). The most extreme dry year of our 1980–2016 study period was 2003, and the most extreme wet year was 2008, and both occurred during a corresponding multiyear wet or dry period (Appendix S1: Table S1).

In multiyear wet periods, JRN experienced higher Pa with lower standard deviation compared to regional Pa (0–500 km; Table 3). In multiyear dry periods, JRN had higher Pa (i.e., was relatively less dry) in 2000–2003 and lower Pa in 2009–2011 compared to regional Pa (Table 3). Despite differences in the mean, the percentile distribution of JRN Pa was strongly correlated to

the 0–500 km Pa distribution from 25th to 75th percentiles in all years, excluding the 2006 and 2008 extremes (r values > 0.75; Fig. 5). Thus, differences in local-regional Pa were produced by the extrema of the local and regional PPT distribution in each year. In support of this finding, JRN Pa differed in direction (above-average versus below-average) from regional Pa in only two years that were part of a multiyear period (1993, 2010; Appendix S1: Table S1).

Local-regional vegetation responses

Maximum growing season NDVI was lower on average at JRN compared to the Chihuahuan Desert region in every year from 1984 to 2016 (Figs. 2b, 6). In average years, JRN NDVI was 90% similar to regional values from 10th to 65–75th percentiles from 0 to 200 km (60% NDVI similarity in total), and from 5th to 35th percentiles from 200 to 500 km (46% similarity in total; Fig. 7). Local-regional similarity from 0 to 200 km during the 1990–1993 wet period was initially low in 1990 (45% similarity in total) and increased to a maximum of 89% similarity in total in 1992 as JRN and regional NDVI increased (Fig. 8; Appendix S1: Table S1). Maximum NDVI was artificially low in 2006 and 2008 due to high cloud cover, yet we observed substantial increases in NDVI in unaffected cells suggest that NDVI similarity was likely high from 0 to 200 km (Figs. 6, 9; Appendix S1: Table S1). Supporting this determination, local-regional NDVI similarity from 0 to 200 km was 90% in 2007 (Fig. 9).

The multiyear dry periods of our study experienced lower maximum NDVI and lower NDVI variance compared to wet periods, and both periods affected the entire 0–500 km region (Fig. 6). Local-regional correlation was much higher than average throughout the 2000–2003 multiyear dry period, with JRN values 90% similar to regional values across a broad range of percentiles (0–200 km: 90% similarity in total; 0–500 km: 75% similarity in total). JRN NDVI was actually higher than regional NDVI in 2000 from 5th to 40th percentiles (Fig. 10). In 2009–2011, JRN NDVI was 90% similar to regional values from 5th to 85th percentiles from 0 to 200 km, and from 5th to 50–60th percentiles from 200 to 500 km (0–200 km: 82% similarity in total; 0–500 km: 62% similarity in total; Fig. 11). JRN
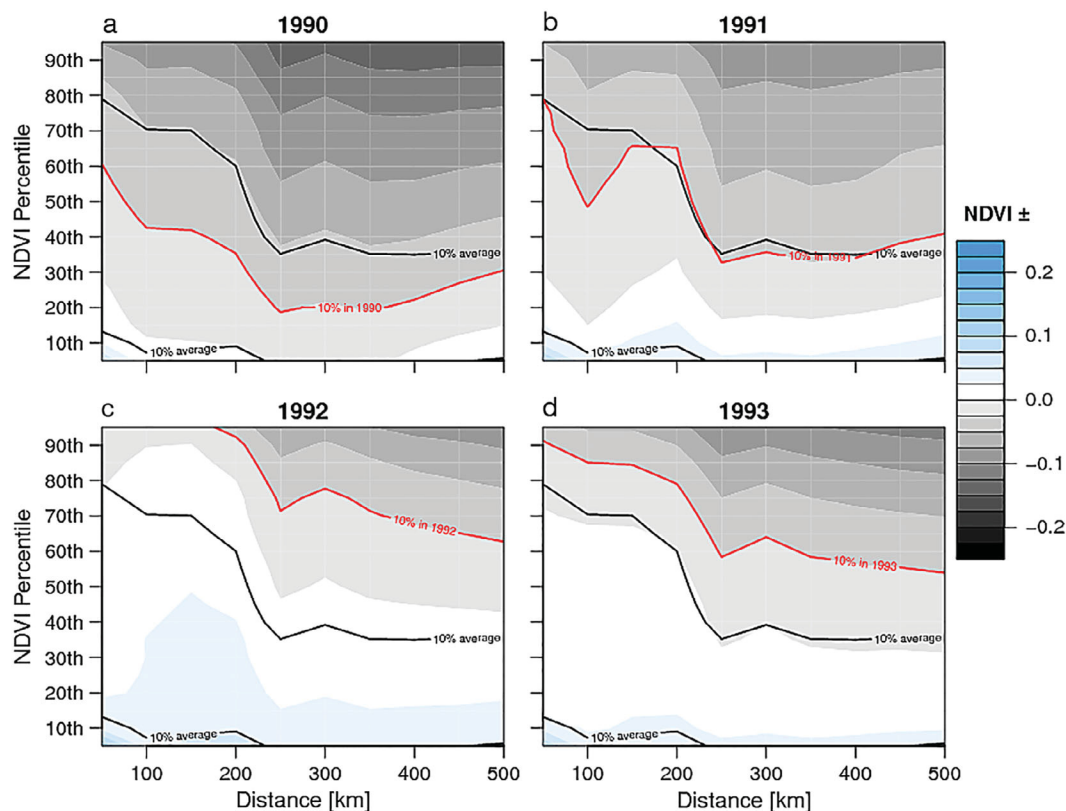
Fig. 8. Plots comparing JRN Normalized Difference Vegetation Index (NDVI) percentiles (5th to 95th) to the same NDVI percentiles from cells 0–50 km to 0–500 km distance from JRN for the 1990–1993 wet period (Wet 1). The color ramp indicates the modified version of Mielke's *r*. The red line indicates the threshold above which JRN and regional cells have less than ~90% similarity, and the black lines illustrate the thresholds above and below which JRN and regional cells have less than ~90% similarity in average years (i.e., not part of a multiyear wet or dry period; see Fig. 6). Years where the red line is above the black lines indicate greater correlation between JRN and regional cells, compared to average relationships.

experienced below-average PPT in 2010, whereas the entire 0–500 km region experienced above-average PPT (Appendix S1: Table S1), and NDVI similarity in this year is lowest of all multiyear dry years (0–500 km: 46% similarity in total; Fig. 11).

DISCUSSION

Local-regional PPT relationships in average years compared to those in multiyear periods

In the Chihuahuan Desert, PPT often alternates between above- and below-average growing seasons of 1–2 yr in length, is spatially and temporally heterogeneous, and rarely approaches mean values (Petrie et al. 2014). Although observation

at a single location is a poor predictor of even localized PPT patterns (Petrie et al. 2014), we found that local PPT estimated from a spatial dataset was a strong predictor of the regional PPT distribution and was a poor fit only when extreme PPT pulses were concentrated over a subregional area in 2006 and 2008. This result differs from our hypothesis and suggests that either distributed PPT estimates may be extended to the larger Chihuahuan Desert region in most years, or that gridded rainfall maps that are interpolated between rain gauges are necessarily spatially autocorrelated and therefore do not fully capture fine-scale variation.

A useful extension of the PPT research in our study would be to leverage meteorological
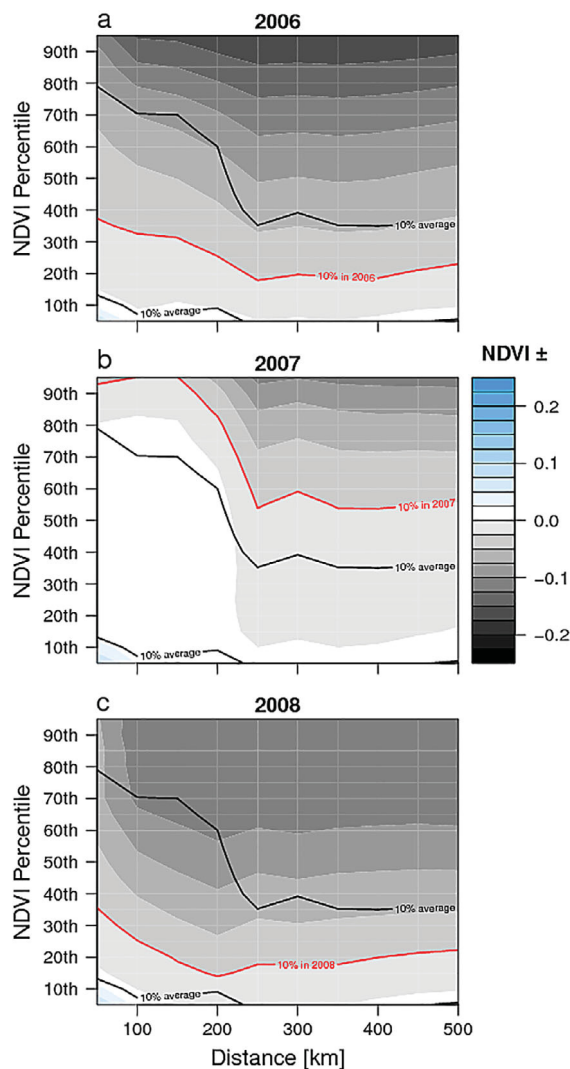
Fig. 9. Plots comparing JRN Normalized Difference Vegetation Index (NDVI) percentiles (5th to 95th) to the same NDVI percentiles from cells 0–50 km to 0–500 km distance from JRN for the 2006–2008 wet period (Wet 2).

sensor networks to refine and enhance accuracy in spatial PPT estimates between research sites such as JRN and larger regional areas. Site-focused, distributed meteorological networks are not often fully incorporated into derived spatial data products, yet these finely distributed meteorological networks could be used to both validate and sharpen local-regional PPT estimates, perhaps using a local-regional neural network approach (Hsu et al. 1997). By doing so, it would

be possible to identify where highly characterized research locations such as those at JRN fall within both the local and regional PPT distribution, and to improve regional prediction of PPT properties (such as rainfall event timing, magnitude, and intensity) by comparing these fine-scale patterns spatially between study areas of differing size.

Local-regional NDVI relationships in average years compared to those in multiyear periods

We found that local-regional NDVI similarity was highest from 0 to 200 km distance. Similarity increased in both multiyear wet and dry periods; the similarity in total was 60 and 45% (0–200 km and 0–500 km, respectively) in average years, and increased to an average of 72 and 57% in the 1990–1993 multiyear wet period, and to an average of 86% and 69% in multiyear dry periods. This pattern supports our hypothesis that local-regional similarity increases in multiyear wet and dry periods. Related studies across multiple semiarid and dryland grassland and shrubland sites suggest that multiyear wet periods have increasing, aggregate effects on vegetation responses through time, whereas dry periods impose a contrasting condition of very low vegetation responses over multiple years (Sala et al. 2012, Petrie et al. 2018). We observed the same pattern at the broader scales of our study; NDVI similarity increased over the 1990–1993 wet period from 0 to 200 km, but we did not observe a temporal pattern in either multiyear dry period. In contrast to our hypothesis, we also did not find a clear effect of the 2003 extreme dry year, which occurred in the last year of a 4-yr period and produced the lowest observed NDVI values of our study. The highest NDVI similarity in total occurred in 2007 (90%), and we expect that this similarity remained high in the extreme 2008 wet year. Although we cannot summarize the effects of extreme wet and dry pulses based on the limited number of events we observed, our study suggests that they may intensify NDVI responses during multiyear wet and dry periods, but may only increase local-regional similarity in wet periods. We found that the effects of dry multiyear periods in our study area are best observed as a temporal aggregate of similar low NDVI conditions, whereas the temporal pattern of increasing NDVI in multiyear wet periods
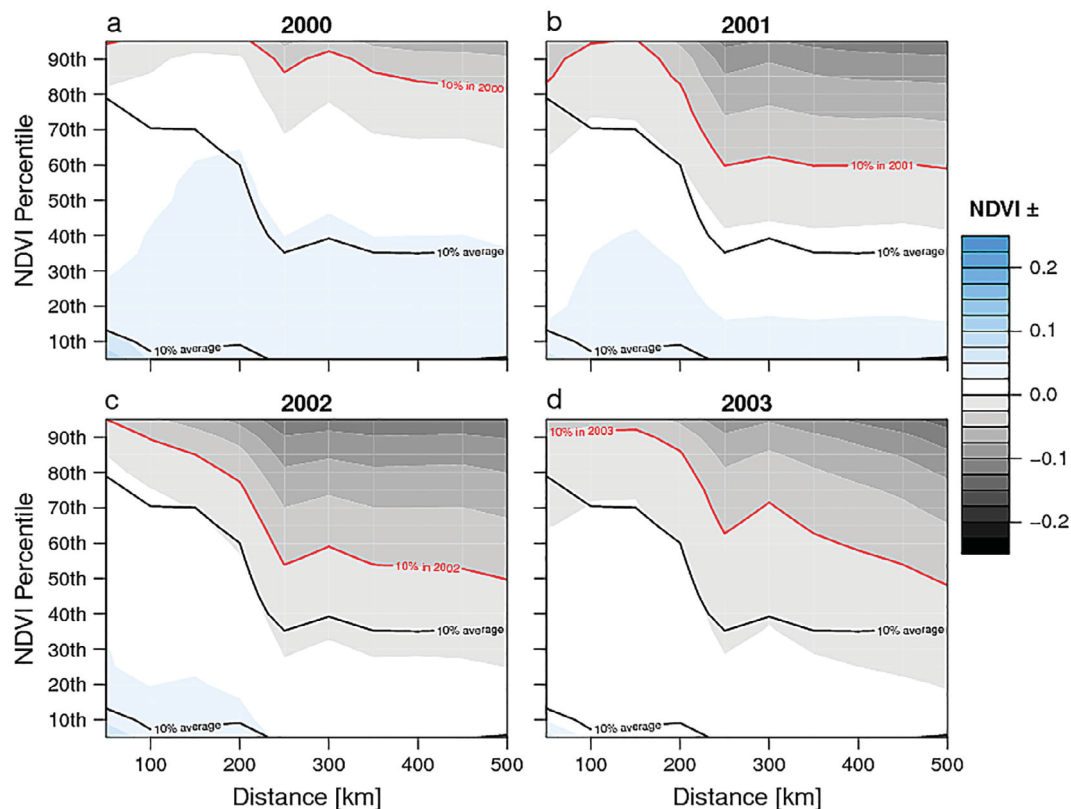
Fig. 10. Plots comparing JRN Normalized Difference Vegetation Index (NDVI) percentiles (5th to 95th) to the same NDVI percentiles from cells 0–50 km to 0–500 km distance from JRN for the 2000–2003 dry period (Dry 1).

suggests that these periods are best studied from year to year.

JRN NDVI is lower than that of the Chihuahuan Desert region on average, which underscores the importance of site and setting when extending local observation to a larger area. One possible reason for lower JRN NDVI is soil characteristics, which underlie vegetation types and states in drylands (Duniway et al. 2010*a*, 2018). In the Chihuahuan Desert, vegetation productivity and proportional transpiration are highest on fine-textured soils with high clay content and water holding capacity (Turnbull et al. 2010), and these soils support higher grass recovery during favorable climatic periods (Duniway et al. 2010*b*). We found that clay content in JRN cells was lower than that of the larger region (JRN: 23%, 0–500 km: 29%), and JRN soils have higher hydraulic conductivity (JRN: 10.7 mm/h, 0–500 km: 6.3 mm/h), likely resulting in lower plant available water (not shown). Additionally,

large grassland areas in the Chihuahuan Desert region have been degraded over the past 100 yr due to multiple disturbances (U.S. Bureau of Land Management 2017), reducing vegetative cover and NDVI (Alvarez et al. 2011, Browning and Steele 2013). Severe degradation events at JRN occurred following overgrazing in the late 1800s and early 1900s and during a severe drought in the 1950s (Gosz and Gosz 1996, Bestelmeyer et al. 2011, Moreno-de las Heras et al. 2016). The recovery time for desert grasslands following degradation events is not yet fully clear (Drewa et al. 2006, Parmenter 2008), and requisite soil stability is actually still increasing at many JRN locations. We found that local-regional similarity at high NDVI percentiles (>70–95th) tended to be low even in cases where NDVI similarity was otherwise very strong (see Fig. 7b). This finding underscores the need to understand if JRN vegetation communities or their responses differ from those across the
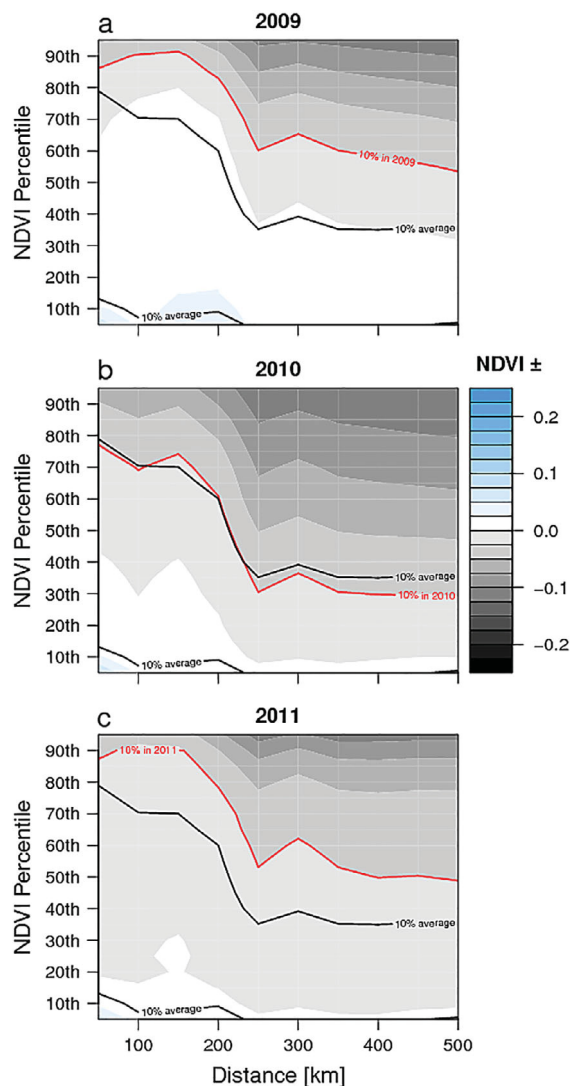
Fig. 11. Plots comparing JRN Normalized Difference Vegetation Index (NDVI) percentiles (5th to 95th) to the same NDVI percentiles from cells 0–50 km to 0–500 km distance from JRN for the 2009–2011 dry period (Dry 2).

Chihuahuan Desert region and to determine if the legacy of degradation underlies the differences we observed.

On the future distribution of multiyear periods

Our study provides an analysis of climatological and ecological patterns that focuses on multiyear PPT periods and shows that these periods have the shared trait of reducing regional heterogeneity in PPT and NDVI, which contrasts with the variable PPT and NDVI conditions this region normally experiences. Multiyear wet periods are critical for herbaceous vegetation recovery and expansion, which are supported by both PPT and favorable landscape conditions (Peters et al. 2012). The second part of this research shows that, for the same wet periods and geographic areas of our study, PPT and soil conditions are the primary factors governing both local and regional vegetation responses and will likely support similarity in spatial vegetation responses between differing future forcing scenarios of high PPT (Petrie et al. 2019). This suggests that there is similarity in the patterns of vegetation responses and the factors supporting them between JRN and the Chihuahuan Desert region, and reinforces the importance of multiyear wet periods. In a changing climate, the pattern and structure of multiyear PPT periods (wet versus dry, mean changes versus extreme pulses) will play an important role in determining the future responses of vegetation in the Chihuahuan Desert.

Conclusions

Comparison of precipitation and vegetation response distributions supports the extension of local, site-based insight across broad regional areas, and analysis of changing local-regional similarity during multiyear wet and dry periods portends to the similar and differing effects these periods have on vegetation responses. We found that multiyear periods of high and low PPT both reduced inherent dryland PPT variability across space and through time, resulting in high local-regional PPT correlation. Multiyear periods also increased local-regional NDVI similarity, although it is clear that additional factors shape vegetation responses. The majority of multiyear wet and dry periods displayed similar response patterns across the entire 500 km^2 study area, with the exception of a period punctuated by extreme wet years, which had strong localized effects on PPT and NDVI that differed in magnitude, geographic area, and timing from other periods. Site-based research may often capture the regional pattern of multiyear PPT periods and in some cases regional vegetation responses as well, and there is opportunity to enhance prediction of precipitation effects associated with

climate change through the extension of local observations and focus on multiyear periods.

Acknowledgments

Literature Cited

Alexander, M., I. Blade, M. Newman, J. Lanzante, N. Lau, and J. Scott. 2002. The atmospheric bridge: The influence of ENSO teleconnections on air-sea interaction over the global oceans. Journal of Climate 15:2205–2231.

Alvarez, L. J., H. E. Epstein, J. Li, and G. S. Okin. 2011. Spatial patterns of grasses and shrubsin an arid grassland environment. Ecosphere 2. https://doi.org/10.1890/ES11-00104.1

Bestelmeyer, B., et al. 2011. Analysis of abrupt transitions in ecological systems. Ecosphere 2. https://doi.org/10.1890/ES11-00216.1

Breshears, D. D., O. B. Myers, C. W. Meyer, F. J. Barnes, C. B. Zou, C. D. Allen, N. G. McDowell, and W. T. Pockman. 2009. Tree die-off in response to global change-type drought: mortality insights from a decade of plant water potential measurements. Frontiers in Ecology and the Environment 7:185–189.

Breshears, D. D., et al. 2005. Regional vegetation die-of in response to global-change-type drought. Proceedings of the National Academy of Sciences of USA 102:15144–15148.

Browning, D., and C. Steele. 2013. Vegetation index differencing for broad-scale assessment of productivity under prolonged drought and sequential high rainfall conditions. Remote Sensing 5:327–341.

Brunsell, N. A., and C. J. Wilson. 2013. Multiscale interactions between water and carbon fluxes and environmental variables in a Central U.S. Grassland. Entropy 15:1324–1341.

Brunsell, N. A., and C. B. Young. 2008. Land surface response to precipitation events using MODIS and NEXRAD data. International Journal of Remote Sensing 29:1965–1982.

Cayan, D., T. Das, D. Pierce, T. Barnett, M. Tyree, and A. Gershunov. 2010. Future dryness in the southwest US and the hydrology of the early 21st century drought. Proceedings of the National Academy of Sciences of USA 107:21271–21276.

Collins, S., S. Koerner, J. Plaut, G. Okie, D. Brese, L. Calabrese, A. Carvajal, R. Evansen, and E. Nonaka. 2012. Stability of tallgrass prairie during a 19-year increase in growing season precipitation. Functional Ecology 26:1450–1459.

Collins, S., et al. 2014. A multi-scale, hierarchical model of pulse dynamics in arid-land ecosystems. Annual Review of Ecology, Evolution and Systematics 45:397–419.

Cook, B., T. Ault, and J. Smerdon. 2015. Unprecedented 21st century drought risk in the American Southwest and Central Plains. Science Advances 1. https://doi.org/10.1126/sciadv.1400082

Drewa, P., D. Peters, and K. Havstad. 2006. Population and clonal level responses of a perennial grass following fire in the northern Chihuahuan Desert. Oecologia 150:29–39.

Duniway, M., B. Bestelmeyer, and A. Tugel. 2010a. Soil processes and properties that distinguish ecological sites and states. Rangelands 32:9–15.

Duniway, M., K. Snyder, and J. Herrick. 2010b. Spatial and temporal patterns of water availability in a grass-shrub ecotone and implications for grassland recovery in arid environments. Ecohydrology 3:55–67.

Duniway, M., M. Petrie, D. Peters, J. Anderson, K. Crossland, J. Herrick, and H. Monger. 2018. Soil water dynamics at 15 locations distributed across a desert landscape: Insights from a 27-yr dataset. Ecosphere 9:1–36.

Duveiller, G., D. Fasbender, and M. Meroni. 2015. Revisiting the concept of a symmetric index of agreement for continuous datasets. Scientific Reports 6:1–14.

ESRI. 2018. ArcGIS Desktop: Release 10. https://www.esri.com/en-us/home

Estiarte, M., et al. 2016. Few multiyear precipitation-reduction experiments find a shift in the productivity-precipitation relationship. Global Change Biology 22:2570–2581.

Fay, P., J. Carlisle, A. Knapp, J. Blair, and S. L. Collins. 2000. Altering rainfall timing and quantity in a mesic grassland ecosystem: design and performance of rainfall manipulation shelters. Ecosystems 3:308–319.

Foley, J., S. Levis, M. Costa, W. Cramer, and D. Pollard. 2000. Incorporating dynamic vegetation cover within global climate models. Ecological Applications 10:1620–1632.

Forzieri, G., F. Castelli, and E. Vivoni. 2011. Vegetation dynamics within the North American Monsoon region. Journal of Climate 24:1763–1783.

Garcia, E., A. Swann, J. Villegas, D. Breshears, D. Law, S. Saleska, and S. Stark. 2016. Synergistic ecoclimate teleconnections from forest loss in different regions structure global ecological responses. PLOS ONE 11. https://doi.org/10.1371/journal.pone.0165042

Gherardi, L., and O. Sala. 2015. Enhanced interannual precipitation variability increases plant functional diversity that in turn ameliorates negative impact on productivity. Ecology Letters 18:1293–1300.

Gosz, R., and J. Gosz. 1996. Species interactions on the biome transition zone in New Mexico: Response of blue grama (*Bouteloua gracilis*) and black grama (*Bouteloua eripoda*) to fire and herbivory. Journal of Arid Environments 34:101–114.

Gutzler, D., and T. Robbins. 2011. Climate variability and projected change in the western United States: regional downscaling and drought statistics. Climate Dynamics 37:835–849.

Hoover, D., and B. Rogers. 2016. Not all droughts are created equal: the impacts of inter-annual drought pattern and magnitude on grassland carbon cycling. Global Change Biology 22:1809–1820.

Hsu, K., X. Gao, S. Sorooshian, and H. Gupta. 1997. Precipitation estimation from remotely sensed information using artificial neural networks. Journal of Applied Meteorology 36:1176–1190.

Jentsch, A., and C. Beierkuhnlein. 2008. Research frontiers in climate change: Effects of extreme meteorological events on ecosystems. Comptes Rendus Geoscience 340:621–628.

Knapp, A., et al. 2017. Pushing precipitation to the extremes in distributed experiments: recommendations for simulating wet and dry years. Global Change Biology 23:1774–1782.

Lehner, F., C. Deser, I. Simpson, and L. Terray. 2018. Attributing the US Southwest's recent shift into drier conditions. Geophysical Research Letters 45:6251–6261.

Mendez-Barroso, L. A., E. R. Vivoni, C. J. Watts, and J. C. Rodriguez. 2009. Seasonal and interannual relations between precipitation, surface soil moisture and vegetation dynamics in the North American monsoon region. Journal of Hydrology 377:59–70.

Mesple, F., M. Troussellier, C. Casellas, and P. Legendre. 1996. Evaluation of simple statistical criteria to qualify a simulation. Ecological Modelling 88:9–18.

Moreno-de las Heras, M., L. Turnbull, and J. Wainwright. 2016. Seed-bank structure and plant-recruitment conditions regulate the dynamics of a grassland-shrubland Chihuahuan ecotone. Ecology 97:2303–2318.

Mueller, B., and S. Seneviratne. 2012. Hot days induced by precipitation deficits at the global scale. Proceedings of the National Academy of Sciences of USA 109:12398–12403.

Notaro, M., and D. Gutzler. 2012. Simulated impact of vegetation on climate across the North American monsoon region in CCSM3.5. Climate Dynamics 38:795–814.

Parmenter, R. 2008. Long-term effects of a summer fire on desert grassland plant demographics in now Mexico. Rangeland Ecology & Management 61:156–168.

Peters, D., J. Yao, D. Browning, and A. Rango. 2014. Mechanisms of grass response in grasslands and shrublands during dry or wet periods. Oecologia 174:1323–1334.

Peters, D., J. Yao, O. Sala, and J. Anderson. 2012. Directional climate change and potential reversal of desertification in arid and semiarid ecosystems. Global Change Biology 18:151–163.

Petrie, M., S. Collins, D. Gutzler, and D. Moore. 2014. Regional trends and local variability in monsoon precipitation in the northern Chihuahuan Desert, USA. Journal of Arid Environments 103:63–70.

Petrie, M., D. Peters, N. Burruss, W. Ji, and H. Savoy. 2019. Differing climate and land-scape effects on regional dryland vegetation responses during wet periods allude to future patterns. Global Change Biology 25:3305–3318.

Petrie, M., et al. 2018. Regional grassland productivity responses to precipitation during multi-year above- and below-average rainfall periods. Global Change Biology 24:1935–1951.

Pineiro, G., S. Perelman, J. Guerschman, and J. Paruelo. 2008. How to evaluate models: Observed vs. predicted or predicted vs. observed? Ecological Modelling 216:316–322.

R Development Core Team. 2016. R: A language and environment for statistical computing. R Foundation for Statistical Computing, Vienna, Austria. http://www.R-project.org

Sala, O., R. Golluscio, W. K. Lauenroth, and P. Roset. 2012. Contrasting nurient-capture strategies in shrubs and grasses of a Patagonian arid ecosystem. Journal of Arid Environments 82:130–135.

Scott, R., J. Biederman, E. Hamerlynck, and G. Barron-Gafford. 2015. The carbon balance pivot point of southwestern US semiarid ecosystems: Insights from the 21st century drought. Journal of Geophysical Research: Biogeosciences 120:2612–2624.

Stark, S., et al. 2016. Toward accounting for ecoclimate teleconnections: intra- and inter-continental consequences of altered energy balance after vegetation change. Landscape Ecology 31:181–194.

Sternberg, L. 2001. Savanna-forest hysteresis in the tropics. Global Ecology and Biogeography 10:369–378.

Swetnam, T., and J. Betancourt. 1998. Mesoscale disturbance and ecological response to decadal climatic variability in the American Southwest. Journal of Climate 11:3128–3147.

Turnbull, L., J. Wainwright, and R. Brazier. 2010. Changes in hydrology and erosion over a

transition from grassland to shrubland. Hydrological Processes 24:393–414.

U.S. Bureau of Land Management. 2017. Chihuahuan Desert rapid eco-regional assessment. U.S. Department of the Interior, Carlsbad, New Mexico, USA.

Williams, A. P., et al. 2002. The atmospheric bridge: the influence of ENSO teleconnections on air-sea interaction over the global oceans. Journal of Climate 15:2205–2231.

Zhang, L., B. Wylie, L. Ji, T. Gilmanov, L. Tieszen, and D. Howard. 2011. Upscaling carbonfluxes over the Great Plains grasslands: Sinks and sources. Journal of Geophysical Research Biogeosciences 116. https://doi.org/10.1029/2010JG001504

SUPPORTING INFORMATION

Additional Supporting Information may be found online at: http://onlinelibrary.wiley.com/doi/10.1002/ecs2.2939/full